Available online at www.sciencedirect.com
ScienceDirect
Renewable and Sustainable Energy Reviews
12 (2008) 1692–1711
RENEWABLE & SUSTAINABLE ENERGY REVIEWS
www.elsevier.com/locate/rser

Potential contribution of wind farms to damp oscillations in weak grids with high wind penetration

R.D. Fernández[a,b,c,*], R.J. Mantz[b,d], P.E. Battaiotto[b]

[a] Universidad Nacional de la Patagonia San Juan Bosco, Argentina
[b] Universidad Nacional de La Plata, Argentina
[c] Laboratorio de Electrónica Industrial, Control e Instrumentación (LEICI), Facultad de Ingeniería, P.O. Box 91, 1900 La Plata, Argentina
[d] Comisión de Investigaciones Científicas de la Provincia de Buenos Aires (CICpba), Argentina

Received 27 November 2006; accepted 9 January 2007

Abstract

In Argentinean Patagonia, there exists a growing interest in understanding local problems associated with the increasing of wind energy penetration in the grid. Recent papers show that some of these power quality problems can be reduced by the proper control of the wind farms. In this way, this work deals with the impact and potential contribution of wind generation on the damping of the electromechanical oscillations called inter- and intra-area oscillations. For gaining qualitative insights and understandings on this complex subject, a test system that allows to isolate the oscillations modes is considered. The analysis shows that new control concepts for wind farm can efficiently contribute to the power system damping.

Keywords: Wind farms; Electromechanical oscillations; Weak grids; Eigenvalue analysis

Contents

*Corresponding author. Laboratorio de Electrónica Industrial, Control e Instrumentación (LEICI), Facultad de Ingeniería, P.O. Box 91, 1900 La Plata, Argentina. Tel./fax: +54 0221 4259306.
E-mail addresses: dfernandez@ing.unlp.edu.ar, dfernandez@unpata.edu.ar (R.D. Fernández).

1364-0321/$ - see front matter © 2007 Elsevier Ltd. All rights reserved.
doi:10.1016/j.rser.2007.01.013

1. Introduction

From early times many countries have been modifying their legislation in order to promote the development of renewable energy. Then, political and economical incentives tend to encourage active power generation as much as possible from wind farms. As examples, green certificates, different kinds of tax exemptions and financial helps to the wind power generation are applied in Chubut State (Argentine) where the biggest argentinean wind farm is located.

However, as the number and size of wind farms increase, the interaction between wind farms and grids becomes more important [1–4]. Then, associated with the total amount of power connected to a distribution network, some power quality problems can arise due to the fluctuating nature of the wind, e.g. voltage and power disturbances which deteriorates the network performance. This fact, which has limited the wind farm installations, is potentiated in weak grids in the southern tip of South America in Patagonia, where the electrical network is not connected to the main interconnected argentinean power system and where the medium wind velocities can be over 12 m/s [5].

These characteristics have generated in Patagonia the necessity of studying the impact of wind generation on electrical networks and researching about the potential contribution of wind farms to overcome some network problems. In this way, this work resumes studies which show how the wind farm control could contribute in one of the aspects of power quality: the damping of electromechanical oscillations.

Oscillations are undesirable because they limit power transfers on transmission lines and, in some cases, induce stress in the mechanical shaft of synchronous generators [6]. These oscillations are of two types [6,7]:

- Local mode or intra-area oscillations. They are associated with rotor angle oscillations, of a single generator or a single plant against the rest of the power system. They usually have frequencies from 1 to 3 Hz.

- Global mode or inter-area oscillations. They involve oscillations of a group of generators in one area against a group of generators in another area. Inter-area oscillations are in the range of less than 1 Hz.

In conventional networks (i.e. without renewable energy resources contribution), small signal analysis and control are well-established techniques [6–8]. These techniques are employed in this work looking for obtaining indexes which allow to evaluate the potential contribution of wind farms for damping electromechanical oscillations. The analysis considers different percentages of wind power penetrations and different kinds of basic control strategies. Simulations are presented to support the analytical results.

The structure of this paper is as follows. In Section 2, a wind farm model is presented. In Section 3, the wind farm model is included in the reference frame of a power system model. Section 4 presents the wind farm control which considers different strategies, particularly it includes simple control strategies to regulate frequency and voltage. In Section 5, the impact of wind farms in a power system is evaluated through an eigenvalue study, and simulation results are carried out. Finally, in Section 6 conclusions are presented.

2. Model of a wind farm

A complete model of a wind farm with a high number of windmills may lead to compute an excessive and impractical number of equations. The size of the wind farm model may be reduced by aggregating several wind turbines with similar incoming wind into a bigger turbine called aggregated turbine [9]. The mechanical and electric parameters per unit are preserved, and the nominal power is increased up to the sum of the nominal power of the whole set of turbines to obtain the parameters of the aggregated turbine.

Making a decision about how many turbines should be aggregated depends on each particular case. Analyzing network changes far from the wind farm, it could be enough to study the wind farm as an only one aggregated turbine. However, when a disturbance takes place in the wind farm it could be necessary the study of all the generators in a separate way [10].

As the main objective of this paper is to examine the effects that the wind farm has over the network oscillations, a single lumped mass of the aggregated wind turbine is considered [11–13]:

$$\left(J_{\mathrm{g}}+\frac{J_{\mathrm{t}}}{N^{2}}\right)N\dot{\Omega}_{\mathrm{t}}=\left(J_{\mathrm{g}}+\frac{J_{\mathrm{t}}}{N^{2}}\right)\dot{\Omega}_{\mathrm{r}}=\frac{T_{\mathrm{t}}}{N}-T_{\mathrm{e}}, \tag{1}$$

which is referred to generator shaft by the gearbox transmission N, being J_{t} and J_{g} the inertias of the aggregated wind turbine and the generator plus the gearbox one, and Ω_{t} and Ω_{r} generator and turbine speeds, respectively. T_{t} is the turbine torque (Appendix A):

$$T_{\mathrm{t}}=\frac{\pi\rho r^{2}}{2}v^{3}C_{\mathrm{p}}(\lambda)/\Omega_{\mathrm{t}}, \tag{2}$$

and T_{e} is the generator torque defined in Appendix B. Because of in Patagonia most of the wind generators are powered by double fed induction (wound rotor) generators (DFIGs), in this work these electric machines are the only ones considered, even when the conclusions can be applied to other variable speed generators. Due to the electric dynamics is fast against that one of the rest of the system [14,15], the dynamical aggregated model of a wind farm can be approximated by the corresponding mechanical behavior.

3. Power system model

The linearized differential–algebraic (DAE) model for a conventional multimachine power system (without wind farms) is [6]

$$\Delta\dot{x} = A_1\Delta x + B_1\Delta I_{\rm g} + B_2\Delta V_{\rm g} + E_1\Delta u, \tag{3}$$

$$0 = C_1\Delta x + D_1\Delta I_{\rm g} + D_2\Delta V_{\rm g}, \tag{4}$$

$$0 = C_2\Delta x + D_3\Delta I_{\rm g} + D_4\Delta V_{\rm g} + D_5\Delta V_{\rm l}, \tag{5}$$

$$0 = D_6\Delta V_{\rm g} + D_7\Delta V_{\rm l}, \tag{6}$$

where the expressions (3)–(6) represent synchronous generator dynamics, static stator synchronous generator equations, active and reactive power equations at generator buses and at load ones, respectively; $\Delta I_{\rm g} = [I_{dn} \quad I_{qn}]^{\rm T}$ are generator currents; $\Delta V_{\rm g} = [\theta_n \quad V_n]^{\rm T}$ are phases and amplitudes of voltages at generator buses; $\Delta u = [\omega_{\rm s} \quad T_{\rm Mi} \quad V_{\rm refi}]^{\rm T}$ are the synchronous frequency, mechanical torques and reference voltages, and $\Delta V_{\rm l} = [\theta_n \quad V_n]^{\rm T}$ are phases and amplitudes of voltages at nongenerator buses.

In order to include the wind farm in the electrical network equations (3)–(6), the linearized model of the aggregated DFIG wind farm operated at constant wind speed is calculated from expression (1):

$$\left(J_{\rm g} + \frac{J_{\rm t}}{N^2}\right)\Delta\dot{\Omega}_{\rm r} = \frac{\Delta T_{\rm turb}}{N} - \Delta T_{\rm e} \Rightarrow \frac{2H_{\rm t+g}}{\omega_{\rm rnom}}\Delta\dot{\omega}_{\rm r} = \frac{(K_{\rm turb}/N^2)(2/P)\Delta\omega_{\rm r}}{P_{\rm BASE}/\omega_{\rm rnom}(2/P)} - \frac{\Delta T_{\rm e}}{P_{\rm BASE}/\omega_{\rm rnom}(2/P)}. \tag{7}$$

Eq. (7) is expressed in p.u., being $H_{\rm t+g} = 1/2\,((J_{\rm g} + (J_{\rm t}/N^2))(\omega_{\rm rnom}(2/P))^2)/P_{\rm BASE}$, $\omega_{\rm r}$ the electrical generator speed, $\omega_{\rm rnom}$ the rated electrical generator speed and $P_{\rm BASE}$ the rated power for scaling all equations in per unit. Also, the gain $K_{\rm turb}$ is obtained from Appendix A, taking the derivative of Eq. (16):

$$K_{\rm turb} = \frac{(\pi\rho r^2/2)v^3\Delta C_{\rm p}/\Delta\Omega_{\rm t} - (\pi\rho r^2/2)v^3 C_{\rm pl}}{\Omega_{\rm tl}^2}, \tag{8}$$

where the subscript "l" indicates the linearization point.

In order to model the complete system (with wind farms), it is necessary to modify expressions (5) (or (6) if the wind farm is connected at a nongenerator bus) with the generated active power and to modify expression (3) as a consequence of the new state, the wind farm equivalent speed ($\omega_{\rm r}$). Also, the generator torque takes different expressions depending on the control strategy applied. Then, before proceeding with the model ($\Delta T_{\rm e}$), it is important to analyze the possibilities about the control of the active and reactive powers of the wind farm.

4. DFIG wind farm control strategies

As it is pointed in Appendix B, vector control can drive independently active and reactive powers of DFIG. Then, this work considers the next cases:

- *CP*: Active power control (tracking or regulation) and reactive power control $\Delta Q_e = 0$.
- *FC*: Active power control $\Delta P_{e(\Delta f)}$ (in order to contribute to frequency regulation) and reactive power control $\Delta Q_e = 0$.
- *FCVC*: Active power control $\Delta P_{e(\Delta f)}$ (in order to contribute to frequency regulation) and reactive power control $\Delta Q_{e(V)}$ (voltage control).

4.1. Conventional wind farm strategies (CP)

One of the most conventional modes of operation of wind farms powered with DFIGs has been to track the curve T_{to} (expression (20), Appendix A):

$$T_{to} = \frac{\pi \rho r^2}{2} \left(\frac{r}{\lambda_o} \right)^3 C_{po} \Omega_t^2, \tag{9}$$

thus getting the maximum active power available in steady state: $P_{to} = T_{to}\Omega_t$.

In this operation mode, wind farms disturb the network as the wind velocity changes. Then, given the growing contribution of wind generation in electrical systems the aforementioned strategy of maximizing the power conversion can be unsuitable for some cases. Hence, other strategies are considered such as the wind farm power regulation at a power reference (P_{SC}) [16].

Obviously, no contribution to reject frequency disturbances can be expected from any two previous wind farm control strategies. This is because of the fast power (vector) control which keeps the wind farm power at its reference value.

4.2. DFIG wind farms with frequency control (FC)

In order to develop a corrective action to frequency changes, the next simple modification of the power reference in the DFIG wind farm is evaluated [17]:

$$P_{wf} = P_{SC} + \Delta P_{e(\Delta f)}, \tag{10}$$

$$\Delta P_{e(\Delta f)} = K \Delta f, \tag{11}$$

being P_{wf} the wind farm power reference, P_{SC} the static power reference, and $\Delta P_{e(\Delta f)}$ a variable component of the wind power reference which is proportional to the frequency variation Δf.

In order to assure the proposed control strategy, it is necessary to consider an inertia reserve of the wind farm from operating each wind turbine with a power coefficient C_{p1} lesser than the optimum one (Appendix A). This fact implies that a static power reference $P_{SC} < P_{to}$ must be assigned at the nominal frequency f_o. Consequently, the wind generator has $100 * (C_{po} - C_{p1})/C_{po}\%$ of additional power to contribute to the frequency regulation in steady state. However, it its important to note that during a transient, the wind farm can contribute with the excess of energy available in the rotor inertia.

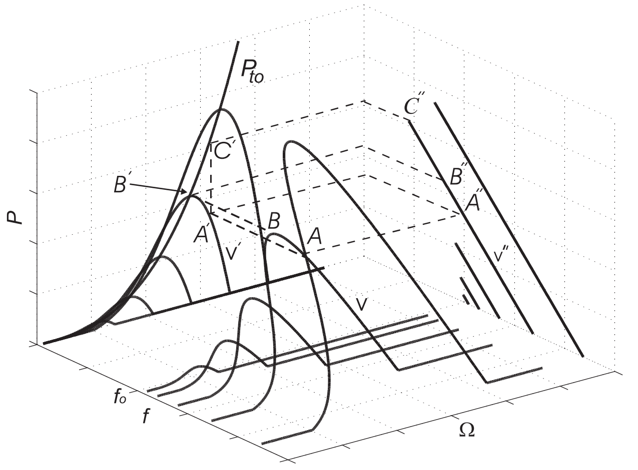


Fig. 1. Power–speed–frequency curves.

Fig. 1 shows power–turbine speed–frequency curves with the wind velocity as a parameter. In particular, wind turbine characteristic curves (expression (17) in Appendix A) are depicted in the power–speed plane, and frequency characteristics are presented in the power–frequency plane. Note that power–frequency characteristics are equivalent to the speed droop characteristics in synchronous generators [8,7], however, the slope of power–frequency characteristics of the FC wind farm can be more pronounced. In this figure the operation point A corresponds to the P_{SC} for nominal frequency f_o and $C_{p1} < C_{po}$. Because of the turbine speed corresponding to the point A' is larger than the turbine speed in point B', there exists an excess of energy stored into the turbine inertia. On the other hand, on each power–frequency characteristic, exist two upper limits, the static limit B'' and the dynamic limit C''. The dynamic limit C'', in correspondence with P_{to}, is specified for preserving the wind farm operation when the frequency remains below its nominal value. Then, it is possible to use the energy in between two curves, the first curve is the turbine speed characteristic P_t and the second one is due to P_{to} which correspond to Eqs. (17) and (19) in Appendix A, respectively.

In the present work, the lower limit considered for the generated power is zero. Then, if frequency increases, the wind farm can reduce its active power injection into the network allowing that the energy can be stored in the inertia, then, all the excess of energy goes to the inertia reserve. Hence:

$$0 \leqslant P_{wf} \leqslant P_{to}. \qquad (12)$$

Contrary to the conventional synchronous generation, double fed induction machines are able to modify very quickly the generated power in comparison with the rest of the electrical system [15]. The aforementioned implies that the participation of the wind farm could be effective, even when the wind power involved would be significantly lesser (for reasons of power quality [10]) than the conventional installed power.

When a DFIG wind farm is operated with FC, expression (7) is modified with:

$$\frac{2H_{\rm t+g}}{\omega_{\rm rnom}}\Delta\dot{\omega}_{\rm r} = \frac{(K_{\rm turb}/N^2)(2/P)\Delta\omega_{\rm r}}{P_{\rm BASE}/\omega_{\rm rnom}(2/P)} - \frac{Kt_{\omega_{\rm e}}\Delta\omega_{\rm e} + Kt_{\omega_{\rm r}}\Delta\omega_{\rm r}}{P_{\rm BASE}/\omega_{\rm rnom}(2/P)}, \tag{13}$$

being $Kt_{\omega_{\rm r}} = -P_{\rm SC}/w_{\rm ro}^2$ and $Kt_{\omega_{\rm e}}$ the FC gain.

Then, for power analysis, expression (5) (or (6)) is modified adding the linearized expression for the FC wind farm:

$$\Delta P_{{\rm e}(\Delta f)} = K_{P\omega_{\rm e}}\Delta\omega_{\rm e}, \tag{14}$$

considering $K_{P\omega_{\rm e}} = Kt_{\omega_{\rm e}}\Omega_{\rm ro}$.

4.3. DFIG wind farms with frequency and voltage control (FCVC)

About the control of the wind farm reactive power $\Delta Q_{\rm e}$, strategies accepted nowadays are:

- $Q_{\rm e}$ regulation, i.e. $\Delta Q_{\rm e} = 0$ (assumed in previous cases);
- $\cos\varphi$ regulation, i.e. $\cos\varphi =$ *specified* [18].

However, taking into consideration the increasing penetration of wind farm generation and looking for satisfying the following objectives [7,19]:

- ○ keeping voltages at the terminals of the equipment within acceptable limits,
- ○ enhancing system stability to maximize utilization of the transmission system,
- ○ minimizing the reactive flow so as to reduce losses ensuring the transmission system operates mainly for active power transfer,
- a DFIG wind farm voltage regulation is evaluated, i.e. $\Delta Q_{\rm e} = \Delta Q_{{\rm e}(V)}$.

Considering active compensation, devices as synchronous compensators and SVCs automatically adjust the reactive power absorbed to maintain voltages of the bus. From this viewpoint, DFIGs with reactive power control can also be considered as active compensation devices.

Taking into account that the wind farm reactive power can be controlled independently of the active one, expression (5) (or (6)) is modified to take into account the voltage control. Here, the most simple case is considered:

$$\Delta Q_{{\rm e}(V)} = K_{QV}\Delta V, \tag{15}$$

being K_{QV} the control gain.

Note that, as with synchronous compensators, the reactive power injection will be limited by the nominal apparent power $S_{\rm n}$ of the DFIG [18].

5. Impact and potential contribution of a wind farm in a power system

5.1. Selected test system

In this section, it is evaluated, how basic control strategies of the DFIG can affect the dynamical behavior of a power system. In this way, Fig. 2 depicts the selected test system.

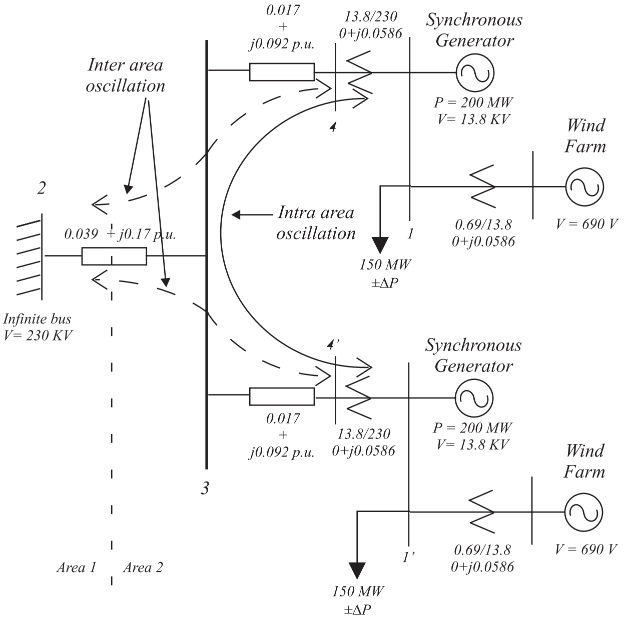


Fig. 2. System under test: inter- and intra-area power flows. Thick line: intra-area oscillation. Dashed line: inter-area oscillation.

It is formed by two areas. Area 1 is an infinite bus meanwhile Area 2 is formed by two synchronous machines in parallel with a wind farm feeding a load which have been considered of constant impedance type. Each synchronous machine, where it is considered a constant motor torque, is associated with a standard IEEE Type I voltage regulator [7].

The symmetrical network topology considered in Fig. 2 is specially chosen for analyzing in a separate way intra- and inter-area oscillations [20]. This topology permits to simplify the analysis by separating the calculus of the network eigenvalues for each oscillation mode.

In Fig. 2, it is considered that the disturbances appear in the loads at buses 1 and/or 1′. It is well known that small signal analysis allows splitting any disturbance input in different components and then to calculate the system response applying the superposition principle [21]. To the ends of the present study it is interesting to split the disturbance input in such a way that:

- one of this new components (named signal or disturbance or fault of common mode [22]) only excites the inter-area oscillation and
- the other component (named signal or disturbance or fault of differential mode [22]) only excites the intra-area oscillation.

In this way, and taking into account the network topology of Fig. 2, any fault at bus 1 and/or 1′ (P_{L1} and $P_{L1'}$, respectively) will be divided in a common load signal [22]:

$$P_{LC} = \frac{P_{L1} + P_{L1'}}{2},$$

which is applied at the same time at both buses 1 and 1′, and a differential load signal: [22]

$$P_{\mathrm{LD}} = \frac{P_{\mathrm{L1}} - P_{\mathrm{L1'}}}{2},$$

applied at the same time in both buses 1 and 1′ but with opposite signs in order to reconstruct P_{L1} and $P_{\mathrm{L1'}}$:

$$P_{\mathrm{L1}} = P_{\mathrm{LC}} + P_{\mathrm{LD}},$$
$$P_{\mathrm{L1'}} = P_{\mathrm{LC}} - P_{\mathrm{LD}}.$$

Note that, in Fig. 2, inter-area oscillations, and no intra-area ones, are obtained from P_{LC} (i.e. the component of fault which is equivalent to two equal signals with the same sign at buses 1 and 1′). In this case both generating groups (synchronous generators and wind farms) behave in the same way respect to the infinite bus, i.e. the synchronous generator shafts experience the same motions indicating that all the Area 2 behaves coherently against the Area 1. Then, the power flow in between the areas corresponds to the indicated in Fig. 2 with dashed lines. As a consequence of the network symmetry and the characteristic of the P_{LC} component of the disturbance, there is no flow in between the synchronous generators (buses 1 and 1′), i.e. there are not intra-area oscillations.

On the other hand, intra-area oscillations can be studied from the differential component of the disturbance which perturbs the network at buses 1 and 1′, the same quantity and at the same time but with opposite signs. Due to the characteristic of P_{LD} and the network topology, the excess of power in one generator group in Area 2 is exactly absorbed by the lack of power on the other generator group in the same area. As a consequence of the power flow, which is depicted in thick line in Fig. 2, there is no variation of the power flow generated/absorbed by the infinite bus, i.e. there are not inter-area oscillations.

Finally, the real response of the system is obtained, by applying the superposition principle, from the addition of the system responses to both components of the disturbance.

5.2. Cases of study. Simulation results

In order to evaluate the power system dynamic behavior when wind power penetration is increased (the same quantity that synchronous generation is decreased), three cases are studied by means of an eigenvalue analysis based on Fig. 2:

1. wind farm with constant active and reactive power regulation (CP), i.e. $\Delta P_{\mathrm{e}} = 0$ and $\Delta Q_{\mathrm{e}} = 0$,
2. wind farm with FC, i.e. $\Delta P_{\mathrm{e}} = \Delta P_{\mathrm{e}(\Delta f)}$ and $\Delta Q_{\mathrm{e}} = 0$,
3. wind farm with frequency and voltage control (FCVC), i.e. $\Delta P_{\mathrm{e}} = \Delta P_{\mathrm{e}(\Delta f)}$ and $\Delta Q_{\mathrm{e}} = \Delta Q_{\mathrm{e}(V)}$.

Fig. 3 presents simulation results for the CP case taking into consideration the selected system in Fig. 2 with a 150 MW load at both buses (1 and 1′) and wind farm and synchronous generations of 30 and 120 MW at each bus, respectively. A disturbance of 40 MW at bus 1 is considered at $t = 2$ s. The transient response of frequency at bus 1 is presented in part (a), this response is separated in intra- and inter-area oscillations in parts

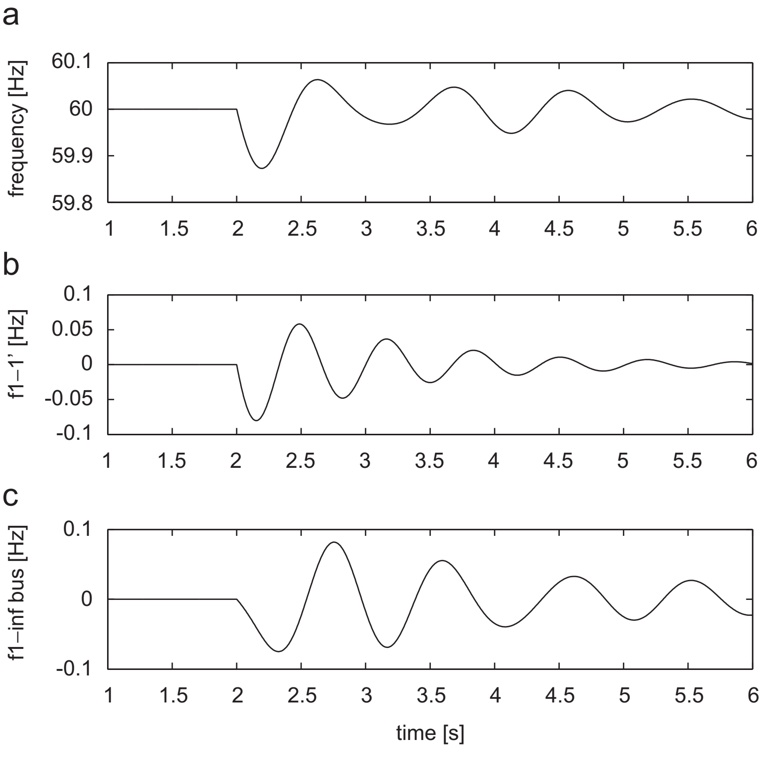


Fig. 3. Dynamic response of the system considering the CP case and a wind farm penetration of 20%: (a) frequency at bus 1, (b) intra-area oscillation and (c) inter-area oscillation.

(b) and (c), respectively. The intra-area oscillation corresponds to the difference between shaft velocities of synchronous generators at buses 1 and $1'$ and the inter-area response is obtained by taking away the inter-area frequency of part (b) from the transient response of frequency of part (a).

In next subsections, the effects of FC and FC and voltage control (FCVC) cases on both kinds of oscillations, intra- and inter-area ones are analyzed and, finally, the total response of the electromechanical oscillation, voltage and control effort are presented.

5.3. *Intra-area oscillations*

Based on the considerations commented in Section 5.1, the eigenvalues corresponding to the intra-area oscillations are calculated and presented in Table 1. Parts (a)–(c) of Table 1 corresponds to CP, FC and FCVC cases, respectively. Note that, looking for emphasizing the problems under study, the eigenvalues, which are scaled by 2π giving frequency in Hz, are calculated for a broad span of wind penetrations.

From analyzing Table 1 it is observed that:

- At the same wind power penetrations, in parts (a)–(c), the most significative differences correspond to the eigenvalues in between lines.

Table 1
Intra-area oscillation

Peol 0 MW	Peol 30 MW	Peol 60 MW	Peol 90 MW	Peol 120 MW	Peol 150 MW
(a) *Case 1: DFIG wind farm with constant power and $Q_e = 0$*					
−157.62	−157.62	−157.62	−157.62	−157.62	−157.63
−4.31	−4.29	−4.27	−4.25	−4.25	−4.25
−2.95	−2.95	−2.94	−2.94	−2.95	−2.95
−0.42	−0.40	−0.39	−0.39	−0.39	−0.39
±1.15i	±1.15i	±1.15i	±1.14i	±1.14i	±1.14i
−0.075	−0.093	−0.108	−0.117	−0.122	−0.123
±1.42i	±1.42i	±1.42i	±1.42i	±1.43i	±1.42i
0	−0.18	−0.18	−0.18	−0.18	−0.18
(b) *Case 2: DFIG wind farm with frequency control and $Q_e = 0$*					
−157.62	−157.62	−157.62	−157.62	−157.62	−157.63
−4.31	−4.34	−4.51	−4.97	−5.96	−6.01
−2.95	−2.95	−2.95	−2.94	−2.95	−2.95
−0.42	−0.41	−0.44	−0.46	−0.43	−0.42
±1.15i	±1.14i	±1.09i	±1.21i	±1.18i	±1.17i
−0.075	−0.17	−0.38	−0.70	−1.05	−1.05
±1.42i	±1.42i	±1.38i	±1.01i	±1.49i	±1.50i
0	−0.18	−0.18	−0.18	−0.18	−0.18
(c) *Case 3: DFIG wind farm with frequency and voltage control*					
−157.62	−157.62	−157.62	−157.62	−157.62	−157.63
−4.31	−4.36	−4.55	−5.02	−6.01	−6.02
−2.95	−3.12	−3.28	−3.35	−3.38	−3.38
−0.42	−0.40	−0.43	−0.45	−0.39	−0.39
±1.15i	±1.13i	±1.06i	±1.21i	±1.05i	±1.04i
−0.075	−0.17	−0.39	−0.70	−1.05	−1.06
±1.42i	±1.42i	±1.37i	±1.03i	±1.49i	±1.50i
0	−0.18	−0.18	−0.18	−0.18	−0.18

Eigenvalue analysis.

- These eigenvalues present, at each wind power penetration, a higher damping factor for the FC and FCVC cases with respect to the CP one. This implies a potential improvement in the damping of the intra-area oscillation for the FC and FCVC cases.
- For each control strategy, the damping of these eigenvalues increases with the wind penetration. This implies that the damping of the intra-area oscillation increases with wind penetration. Again, this increment is much more marked in the FC and FCVC cases.
- In the CP case, the eigenvalues displacement with the increment of the wind energy is not significative. This fact is attributable to the independence of the CP strategy with respect to the frequency and voltage variations. In this case, the eigenvalues movement is a consequence of unloading the synchronous generators with wind penetration, i.e. there is a drop in the load which ''sees'' each synchronous generator provided that more wind energy is injected into the network.

Figs. 4 and 5 show the movement, for different wind energy penetrations, of the aforementioned eigenvalues for the CP and FC–FCVC cases, respectively. Fig. 5 indicates the strong (positive) influence on the damping of the intra-area oscillation with the FC and FCVC control strategies.

Fig. 6 presents, for the three strategies, the intra-area oscillation when takes place a load change in 40 MW at $t = 2$ s at bus 1, being the wind farm power generation and the synchronous power generation of 30 MW and 120 MW at each bus, respectively.

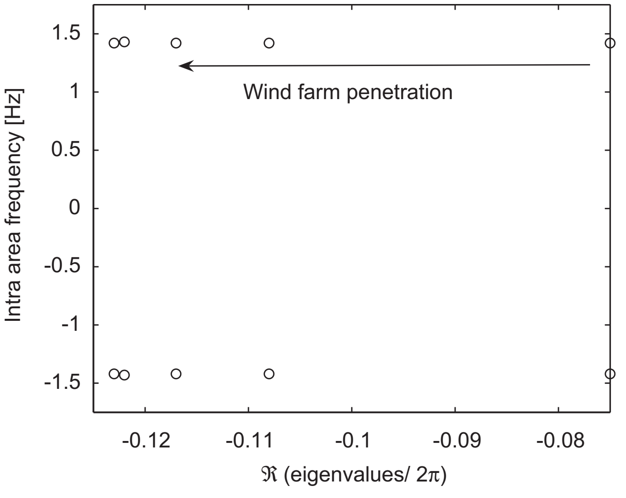


Fig. 4. Intra-area eigenvalues for the CP case at different wind farm penetrations.

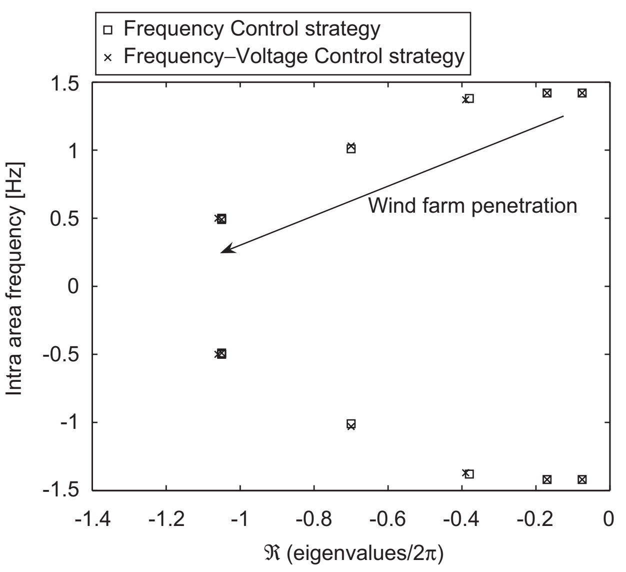


Fig. 5. Intra-area eigenvalues for FC and FCVC cases at different wind farm penetrations.

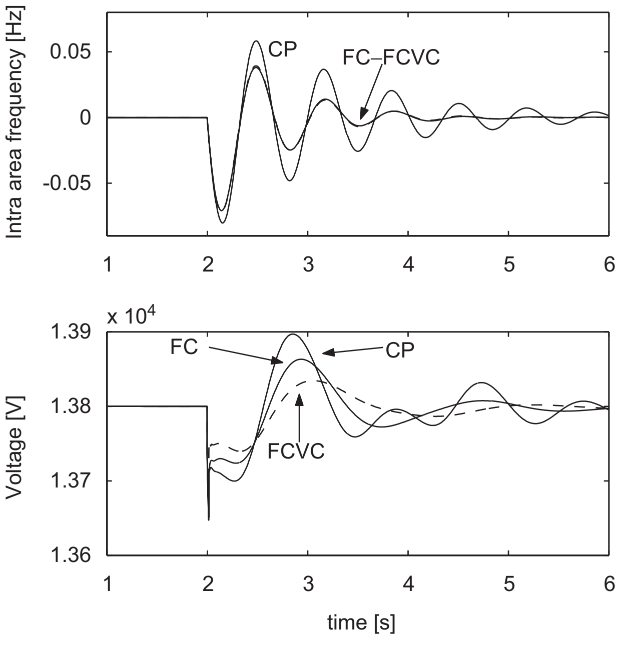


Fig. 6. Intra-area oscillation and voltage at bus 1 with a wind farm penetration of 20%. Wind farm with: constant power (CP), frequency control (FC) and frequency and voltage control (FCVC) strategies.

Simulation results agree with the expected improvements from Table 1 and show the strong impact on the intra-area oscillation of the FC and FCVC control strategies when they are compared with the CP one. At the same time it is observed that the transient behavior of the intra-area mode is almost the same for the FC and FCVC control strategies but the last one, as a consequence of the reactive power loop ($\Delta Q_{e(V)}$), produces a better voltage profile.

5.4. Inter-area oscillations

Table 2 presents, based on the considerations commented in Section 5.1, the eigenvalues corresponding to the inter-area oscillations for the three aforementioned cases.

Analyzing Table 2 the next conclusions (similar to the Table 1) can be obtained:

- Comparing the inter-area eigenvalues for the three control strategies at equal wind power penetrations, the main differences correspond to the eigenvalues in between lines.
- Also, for each case, the damping of these eigenvalues increases with the wind penetration and it is much more marked in the FC and FCVC cases. This is shown in Figs. 7 and 8 where are presented the evolutions of the aforementioned eigenvalues for the CP and FC–FCVC cases, respectively. This implies that the damping of the inter-area oscillation increases with wind penetration.
- These eigenvalues present, at each wind power penetration, a damping factor which is highly superior for the FC and FCVC cases with respect to the CP one. This implies a substantial improvement in the damping of the inter-area oscillation for the FC and FCVC cases.

Table 2
Inter-area oscillation

Peol 0 MW	Peol 30 MW	Peol 60 MW	Peol 90 MW	Peol 120 MW	Peol 150 MW
(a) *Case 1: DFIG wind farm with constant power and* $Q_e = 0$					
−157.62	−157.62	−157.62	−157.62	−157.62	−157.63
−3.76	−3.71	−3.68	−3.66	−3.64	−3.64
−2.70	−2.70	−2.70	−2.71	−2.72	−2.74
−0.49	−0.48	−0.48	−0.48	−0.48	−0.49
±1.46i	±1.47i	±1.48i	±1.49i	±1.50i	±1.50i
−0.039	−0.046	−0.051	−0.056	−0.059	−0.061
±1.00i	±1.00i	±1.00i	±0.99i	±0.99i	±0.99i
0	−0.18	−0.18	−0.18	−0.18	−0.18
(b) *Case 2: DFIG wind farm with frequency control and* $Q_e = 0$					
−157.62	−157.62	−157.63	−157.63	−157.63	−157.63
−3.76	−3.75	−3.90	−2.73	−2.38	−2.36
−2.70	−2.70	−2.71	−1.60	−2.42	−2.41
−0.49	−0.46	−0.46	−0.50	−0.51	−0.51
±1.46i	±1.48i	±1.53i	±1.53i	±1.51i	±1.50i
−0.039	−0.20	−0.58	−4.49	−6.27	−6.38
±1.00i	±0.98i	±0.74i	&−1.60	&−0.23	&−0.23
0	−0.18	−0.18	−0.18	−0.18	0.18
(c) *Case 3: DFIG wind farm with frequency and voltage control*					
−157.62	−157.61	−157.61	−157.60	−157.60	−157.60
−3.76	−3.77	−3.94	−3.34	−3.38	−3.38
−2.70	−3.02	−3.26	−1.70	−2.53	−2.52
−0.49	−0.46	−0.45	−0.47	−0.44	−0.44
±1.46i	±1.46i	±1.47i	±1.38i	±1.27i	±1.26i
−0.039	−0.20	−0.58	−4.51	−6.26	−6.37
±1.00i	±0.98i	±0.74i	&−0.47	&−0.23	&−0.23
0	−0.18	−0.18	−0.18	−0.18	−0.18

Eigenvalue analysis.

Simulation results, presented in Fig. 9, show the inter-area oscillation and the voltage at bus 1. A strong impact on the inter-area oscillation of the FC and FCVC control strategies when they are compared with the CP one is observed. Note that, the inter-area oscillation presents a slightly better behavior for the FC case when it is compared with the FCVC case. However, the last one improves the voltage profile.

5.5. Complete transient response at bus 1

Fig. 10 presents, for the three cases and at bus 1, in part (a) the complete transient response of the frequency, i.e. the shaft oscillation of the synchronous generator at bus 1, in part (b) the voltage and in part (c) the apparent power of the wind farm.

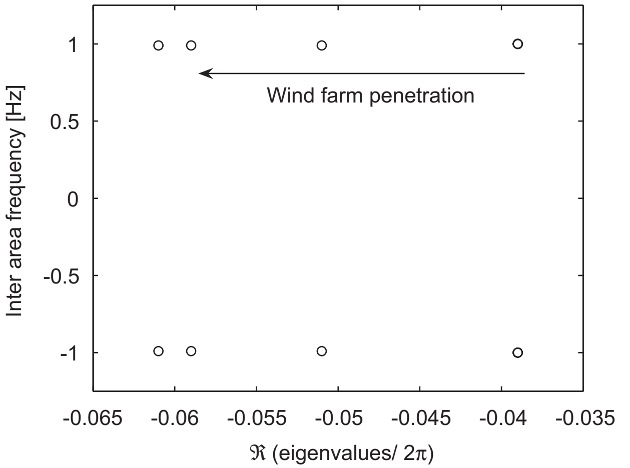


Fig. 7. Inter-area eigenvalues for the CP case at different wind farm penetrations.

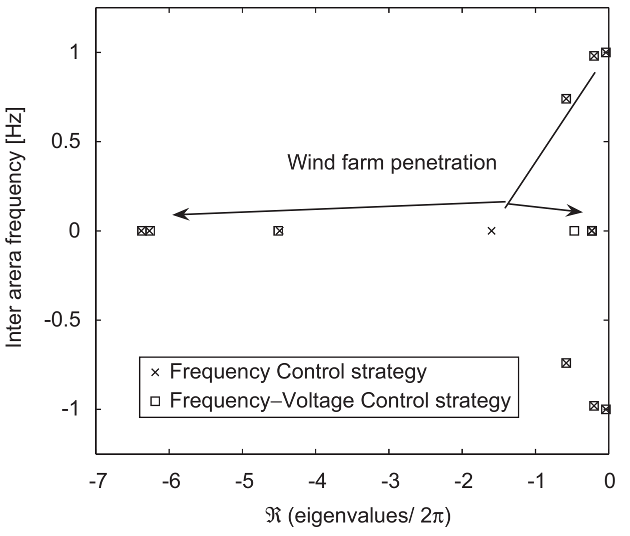


Fig. 8. Inter-area eigenvalues for FC and FCVC cases at different wind farm penetrations.

Parts (a) and (b) of Fig. 10, clearly show the improvements over the transient response of frequency and the voltage for the FC and FCVC cases when they are compared with the CP case. The reactive power loop ($\Delta Q_{e(V)}$) produces in part (a) of Fig. 10 a slight decrease in the performance of the transient response of the frequency with respect to the FC case. This fact is attributable to the lesser variation in the voltage observed in part (b). Indeed, as the voltage changes, constant impedance loads (considered in this work) tends to damp the frequency oscillation by modifying the active power absorbed.

In part (c) of Fig. 10, it is noted that when the disturbance appears, DFIG wind farms with FC and FCVC react carrying out a contribution of active, and active and reactive

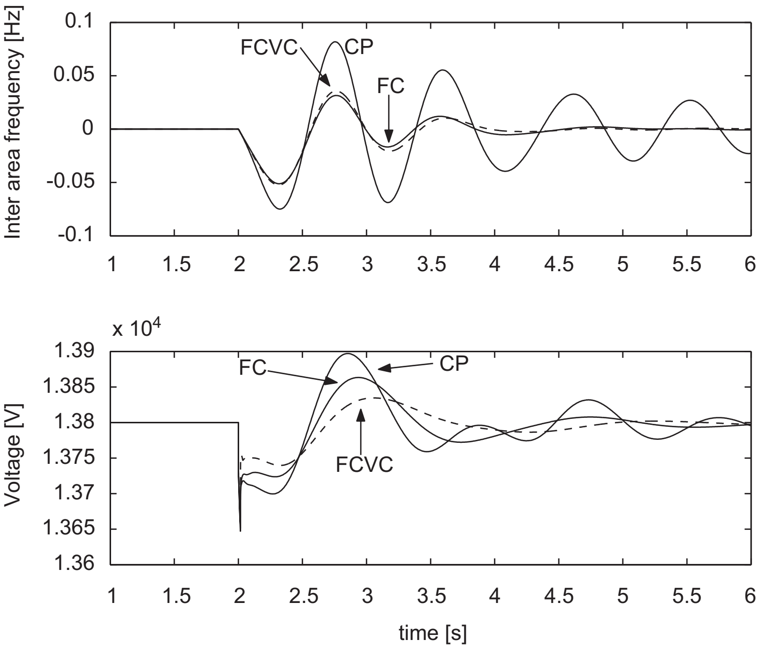


Fig. 9. Inter-area oscillation and voltage at bus 1 with a wind farm penetration of 20%. Wind farm with: constant power (CP), frequency control (FC) and frequency and voltage control (FCVC) strategies.

powers, respectively. The reactive power contribution is corroborated in part (b) where is observed the improvement in the voltage profile. Note, that the maximum (transient) increment of the apparent power, i.e. the control effort involved, is about a fourth part of the steady state condition with less than a half second of duration. However, this is enough to strongly improve the transient response of frequency in part (a) and the voltage response of part (b).

6. Conclusions

In Argentinean Patagonia, there exists an increasing interest in understanding some problems associated with wind power generation. This fact is motivated for particular characteristics of the region as weak grids and high wind speeds. In this way, this work presents studies which show how control strategies of the wind farms could contribute in one of the aspects of power quality: the damping of electromechanical oscillations. Also, considering the apparent power available, a reactive power control strategy which enables to improve the voltage profile at the bus where the wind farm is connected was evaluated.

Three cases were considered, wind farms with conventional power control (constant power: CP), with frequency control (FC) and with frequency control and reactive power control (FCVC).

The analysis of the impact of wind power on the electromechanical oscillations has been done by observing the location of eigenvalues for different wind power penetrations in a test system that allows to isolate the oscillations modes. It was showed that as the wind

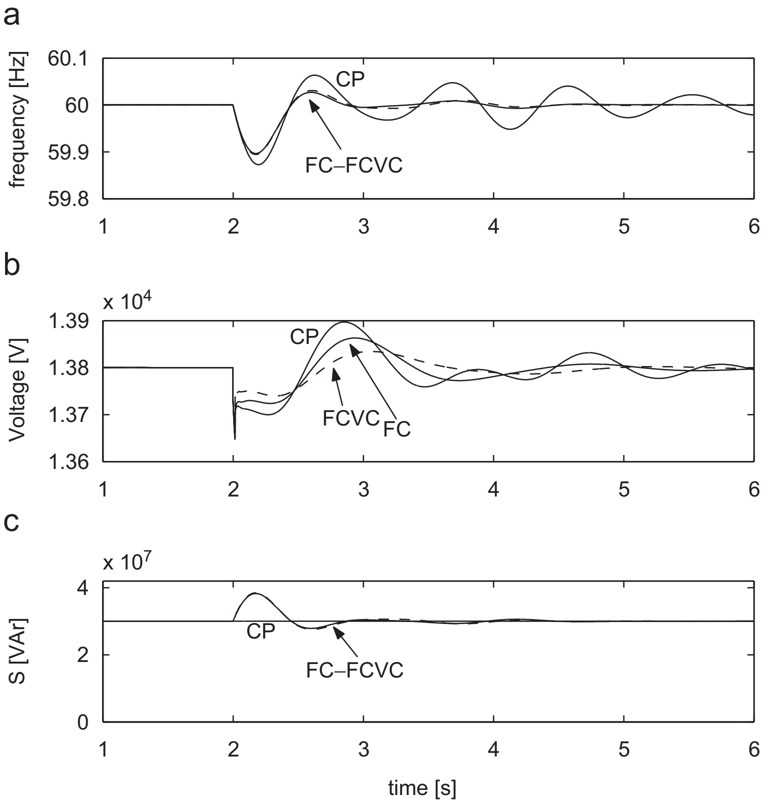


Fig. 10. System response at bus 1 with a wind farm penetration of 20%: (a) frequency, (b) wind farm voltage and (c) apparent power of the wind farm.

power penetration was increased wind farms with FC and with FCVC control strategies highly increased the eigenvalues damping for both kinds of oscillations, inter- and intra-area ones. Then, these strategies contribute to the damping of the electromechanical oscillations. This was corroborated with simulation results. Also, the reactive power control allowed to regulate the voltage with a slight decrease in the performance of the transient response. Also, simulation results showed that, with a reasonable control effort (incremental wind farm apparent power), is possible to highly damp electromechanical oscillations.

Finally, note that, due to the basic characteristic of the control strategies considered, it can be expected that investigations on other network configurations will led to similar results, counteracting adverse effects of high wind energy penetration in power systems.

Acknowledgment

This work was supported by UNLP, UNPSJB, CICpBA, CONICET and ANPCyT.

Appendix A. Wind turbine

The torque and the mechanical power developed by a wind turbine are given by [23]

$$T_t = \frac{\pi\rho r^2}{2} v^3 C_p(\lambda)/\Omega_t, \tag{16}$$

$$P_t = \frac{\pi\rho r^2}{2} v^3 C_p(\lambda), \tag{17}$$

where ρ is the air density, r is the radius of the turbine, v is the wind speed, $C_p(\lambda)$ is the power coefficient, $\lambda = \Omega_t r/v$ is the tip speed ratio and Ω_t is the turbine speed.

Because of C_p is maximum at the optimum tip speed ratio $\lambda = \lambda_o$, to extract the maximum available power at any wind velocity, the control system should adjust the turbine speed to force:

$$\Omega_t = \Omega_{to} = \frac{\lambda_o v}{r}. \tag{18}$$

At this rotational speed the maximum turbine power P_{to} and the corresponding torque T_{to} result:

$$P_{to} = \frac{\pi\rho r^2}{2}\left(\frac{\Omega_t r}{\lambda_o}\right)^3 C_{po}, \tag{19}$$

$$T_{to} = \frac{\pi\rho r^2}{2}\left(\frac{r}{\lambda_o}\right)^3 C_{po}\Omega_t^2, \tag{20}$$

being $C_{po} = C_p(\lambda_o)$ the maximum power coefficient.

Appendix B. Generating units (DFIG)

Variable speed wind farms powered by DFIG (wound rotor) are the only ones considered in this work. The rotor winding is fed using a back-to-back voltage source converter as depicted in Fig. 11.

The operation of an induction machine can be analyzed using the classical theory of rotating fields and the well-known d–q model [24]. In this way, the general reference frame

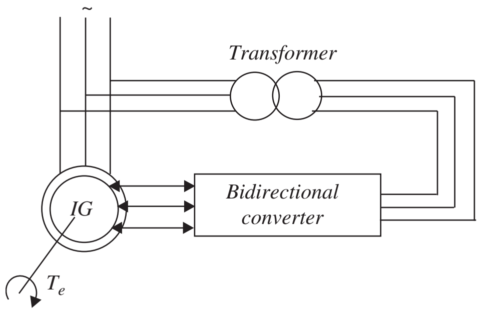


Fig. 11. Generating unit: double fed induction generator (DFIG) with rotor converter for variable speed operation.

model for the induction machine is expressed through the following matrix equation:

$$\begin{bmatrix} u_{sx} \\ u_{sy} \\ u_{rx} \\ u_{ry} \end{bmatrix} = \begin{bmatrix} R_s + pL_s & -\omega_g L_s & pL_m & -\omega_g L_m \\ \omega_g L_s & R_s + pL_s & \omega_g L_m & pL_m \\ pL_m & -(\omega_g - \omega_r)L_m & R_r + pL_r & -(\omega_g - \omega_r)L_r \\ (\omega_g - \omega_r)L_m & pL_m & (\omega_g - \omega_r)L_r & R_r + pL_r \end{bmatrix} \begin{bmatrix} i_{sy} \\ i_{sx} \\ i_{ry} \\ i_{rx} \end{bmatrix}, \tag{21}$$

where L_s and L_r are the stator and rotor inductances, L_m is the magnetizing inductance, R_r and R_s are the stator and rotor side resistances, ω_r is the electrical rotor speed, ω_g is the reference frame speed, u_{sx} and u_{sy} are stator voltages and u_{rx} and u_{ry} are rotor voltages, finally i_{sx}, i_{sy}, i_{rx} and i_{ry} are the stator and rotor currents. If ω_g is equal to the line frequency ω_e, the synchronously rotating reference frame model is obtained.

The electromagnetic torque T_e, the stator active (P_e) and reactive (Q_e) powers of a DFIG are given by

$$T_e = -\tfrac{3}{2} P L_m (i_{sx} i_{ry} - i_{sy} i_{rx}), \tag{22}$$

$$P_e = \tfrac{3}{2}(u_{sx} i_{sx} + u_{sy} i_{sy}), \tag{23}$$

$$Q_e = \tfrac{3}{2}(u_{sy} i_{sx} - u_{sx} i_{sy}), \tag{24}$$

with P the number of poles. Because of vector control, it is possible to control active and reactive powers independently [24,25].

Appendix C

Wind turbine: $P = 700\,\text{kW}$ at $v = 11.75\,\text{m/s}$; $r = 22\,\text{m}$; $\rho = 1.224$; $C_p(\lambda) = 1.206 \times 10^{-5}\lambda^7 - 2.71 \times 10^{-4}\lambda^6 + 2.0399 \times 10^{-3}\lambda^5 - 6.519 \times 10^{-3}\lambda^4 + 1.257 \times 10^{-2}\lambda^3 - 1.54 \times 10^{-2}\lambda^2 + 2.85 \times 10^{-2}\lambda - 4.05 \times 10^{-2}$.

DFIG: $V = 690\,\text{V}$; $R_s = 0.0067\,\Omega$; $P = 4$; $L_s = 0.0075\,\text{Hy}$; $L_m = 0.0061\,\text{Hy}$; $L_r = 0.0084\,\text{Hy}$; $R_r = 0.187\,\text{Hy}$; $a = 0.3806$ turns ratio; $J_{t+mi} = 536096.59\,\text{Kg}\,\text{m}^2$; $N = 51$.

References

[1] Muljadi E, Wan Y, Butterfield CP, Parsons B. A study of a wind farm power system, National wind technology center national renewable energy laboratory golden, Colorado, January 2002. NREL/CP-500-30814. Available electronically at ⟨http://www.osti.gov/bridge⟩.

[2] Muljadi E, Butterfield CP. Wind farm power system model development, World renewable energy congress VIII, Denver, Colorado, August 29–September 3, 2004. NREL/CP-500-36199. Preprint. Available electronically at ⟨http://www.osti.gov/bridge⟩.

[3] Randall G, Vilhauer R, Thompson C. Characterizing the effects of high wind penetration on a small isolated grid in Arctic Alaska. September 2001. NREL/CP-500-30668. AWEA's WINDPOWER 2001 Conference, Washington, DC; June 4–June 7; 2001. Available electronically at ⟨http://www.doe.gov/bridge⟩.

[4] Parsons B, Milligan M, Smith JC, DeMeo E, Oakleaf B, Schuerger M, et al. Grid impacts of wind power variability: recent assessments from a variety of utilities in the United States. NREL/CP-500-39955, July 2006. Available electronically at ⟨http://www.doe.gov/bridge⟩.

[5] CREE, Centro Regional de Energía Eólica. Chubut, Patagonia Argentina. ⟨http://www.eeolica.com.ar/⟩. Accessed September 14, 2006 [in Spanish].

[6] Sauer PW, Pai MA. Power systems dynamics and stability. Englewood Cliffs, NJ: Prentice-Hall; 1998.

[7] Kundur P. Power systems stability and control. New York: McGraw-Hill; 1993.

[8] Elgerd O. Electric energy systems theory: an introduction. New York: McGraw-Hill; 1970.

[9] Ledesma P, Usaola J, Rodríguez J. Transient stability of a fixed speed wind farm. Renew Energy 2002:1341–55.
[10] Ledesma P. Parques eólicos, Tesis de Doctor, Universidad Carlos III, Madrid. España; 2001 [in Spanish].
[11] Ekanayake J, Jenkins N. Comparison of the response of doubly fed and xed-speed induction generator wind turbines to changes in network frequency. IEEE Trans Energy Convers 2004;19(4):800–2.
[12] Mullane A, O'Malley M. The inertial response of induction-machine-based wind turbines. IEEE Trans Power Syst 2005;20(3):1496–503.
[13] Lalor G, Mullane A. Frequency control and wind turbine technologies. IEEE Trans Power Syst 2005;20(4):1905–13.
[14] Ledesma P, Usaola J. Effect of neglecting stator transients in doubly fed induction generators models. IEEE Trans Energy Convers 2004;2:459–61.
[15] Ledesma P, Usaola J. Doubly fed induction generator model for transient stability analysis. IEEE Trans Energy Convers 2005;2:388–97.
[16] Hansen AD, Sørensen P, Iovb F, Blaabjerg F. Power control of wind farm with doubly fed induction generators. Renew Energy. Available online 10 August 2005, [in press].
[17] Fernández R, Mantz R, Battaiotto P. Potential contribution of wind farms to the frequency regulation. Sixth Latin-American congress of electricity generation and transmission, November 13–17, 2005.
[18] Tapia G, Tapia A, Criado R, Saenz J. Voltage regulation of distribution networks through reactive power control. IFAC, 15th triennial world congress, Barcelona, Spain, 2002.
[19] Romanowitz H, Muljadi E, Yinger R. VAR support from distributed wind energy resources, World renewable energy congress VIII, Denver, Colorado, August 29–September 3; 2004. NREL/CP-500-36210. Available electronically at ⟨http://www.osti.gov/bridge⟩.
[20] Slootweg J, Kling W. The impact of large scale wind power generation on power system oscillations. Electr Power Syst Res 2003:9–20.
[21] Oppenhein A, Willsky A. Signals & Systems. Englewood Cliffs, NJ: Prentice-Hall; 1996.
[22] Gray P, Meyer R. Analysis and design of analog integrated circuits. New York: Wiley; 1993.
[23] Freris L. Wind energy conversion systems. Englewood Cliffs, NJ: Prentice-Hall International; 1990.
[24] Vas P. Sensorless vector and direct torque control. Oxford: Oxford University Press; 1998.
[25] Petersson A, Harnefors L, Thiringer T. Comparison between stator-flux and grid-fux-oriented rotor current control of doubly-fed induction generators. 35th Annual IEEE power electronics specialists conference, 2004. p. 482–9.